Orthogonal paper biosensor for mercury(II) combining bioluminescence and colorimetric smartphone detection

Orthogonal paper biosensor for mercury(II) combining bioluminescence and colorimetric smartphone detection

Antonia Lopreside, Laura Montali, Baojun Wang, Annalisa Tassoni, Maura Ferri, Maria Maddalena Calabretta, Elisa Michelini

Biosens Bioelectron 2021 Aug 20;194:113569. doi: 10.1016/j.bios.2021.113569. Online ahead of print.

Cite this article as: Lopreside A, Montali L, Wang B, Tassoni A, Ferri M, Calabretta MM, Michelini E. Orthogonal paper biosensor for mercury(II) combining bioluminescence and colorimetric smartphone detection. Biosens Bioelectron. 2021 Aug 20;194:113569. doi: 10.1016/j.bios.2021.113569.

Orthogonal paper biosensor for mercury(II) combining bioluminescence and colorimetric smartphone detection

Antonia Lopreside[1,2¥], Laura Montali[1,2¥], Baojun Wang[3,4], Annalisa Tassoni[5], Maura Ferri[5,6], Maria Maddalena Calabretta[*1,2] and Elisa Michelini[*1,2,7]

[1] Department of Chemistry "Giacomo Ciamician", University of Bologna, Via Selmi 2, 40126 Bologna, Italy

[2] Center for Applied Biomedical Research (CRBA), Azienda Ospedaliero-Universitaria Policlinico S. Orsola-Malpighi, Bologna, Italy

[3] Centre for Synthetic and Systems Biology, School of Biological Sciences, University of Edinburgh, Edinburgh, United Kingdom

[4] Hangzhou Innovation Center, College of Chemical and Biological Engineering, Zhejiang University, Hangzhou 311200, China

[5] Department of Biological, Geological and Environmental Sciences, University of Bologna, Bologna, Italy

[6] Department of Civil, Chemical, Environmental and Materials Engineering, University of Bologna, Bologna, Italy

[7] Health Sciences and Technologies-Interdepartmental Center for Industrial Research (HST-ICIR), University of Bologna, Bologna, Italy

*Corresponding authors: elisa.michelini8@unibo.it; maria.calabretta2@unibo.it

[¥] These authors contributed equally

Abstract

Mercury contamination in the environment has reached alarming levels. Due to its persistence and bioaccumulation, mercury is one of the most widespread toxic heavy metals found in air, water and food. Thus, it is mandatory to monitor mercury and its compounds, and the availability of sensitive and rapid biosensors is highly valuable.

We developed a low-cost biosensor for orthogonal detection of mercury(II) integrating three different biorecognition principles on a three-leaf paper: i) a mercury-specific bioluminescent *Escherichia coli* bioreporter strain expressing NanoLuc luciferase as reporter protein, ii) a purified β-galactosidase (β-gal) enzyme which is irreversibly inhibited by mercury and other metal ions, and iii) an *Aliivibrio fischeri* bioluminescent strain which is used to quantitatively assess sample toxicity and correct the analytical signal accordingly.

Both sensory elements and substrates, Furimazine for the bioluminescent reporter strain and chlorophenol red-β-D-galactopyranoside for colorimetric detection of β-gal, were integrated in the paper sensor to provide a stable all-in-one disposable cartridge which can be easily snapped into a smartphone with a clover-shaped 3D printed housing. This is the first integration of bioluminescence and colorimetric detection on a smartphone-paper sensor, providing a readout within 15 and 60 min for the colorimetric and bioluminescent detection respectively. The biosensor was applied to water samples spiked with different concentrations of mercury, interferents and toxic chemicals providing a limit of detection for Hg(II) at the ppb levels.

Keywords: bioluminescence, colorimetric, paper sensor, smartphone, mercury

INTRODUCTION

Mercury is a global contaminant that causes severe health effects including neurological and gastrointestinal disorders in humans and wildlife. Contamination of water with mercury and its inorganic and organic compounds is still very frequent in several areas worldwide, deriving from both natural and anthropogenic sources. According to the European Environment Agency, about 41% of EU surface water bodies have a mercury concentration exceeding the safety limits, with alarming cases, such as Sweden, with all surface bodies not meeting the environmental quality standard for mercury in biota (European Commission Report, 2012; Lemm et al., 2021).

Notably, mercury speciation and transport between aqueous and solid phases are responsible for different levels of toxicity. In aquatic environments, such as water bodies, sediments, aquatic flora and fauna, mercury occurs mostly as divalent cation in organic and inorganic complexes and as Hg(0) dissolved in the aqueous phase (Leopold et al, 2010). Due to bioaccumulation phenomenon mercury is also present in food, in particular seafood and dairy products, as reported by EFSA (EFSA, 2015). The Minamata Convention on mercury, supported by the World Health Organization (WHO), entered into force in 2017 providing binding measures, such as the banning of mercury in batteries, thermometers, and light bulbs with the goal of protecting the environment and human health from adverse effects of mercury. Accordingly, it is mandatory to monitor mercury and its compounds in aquatic environments, drinking water and food (European Environment Agency, 2018; Minamata Convention, Progress Report 2020).

Accurate analysis of mercury can be achieved with standard analytical techniques and physico-chemical methods that are generally expensive, not suitable for on-site analysis and require non-green procedures. Cost-effective and eco-friendly methods that enable a rapid and on-site analysis are highly valuable to prioritize samples that need to undergo a more accurate analysis

(Calabretta et al., 2021). This would enable a more capillary and widespread screening of water samples and reduce the number of samples to be sent to specialized laboratories for confirmatory analysis. Different biosensors were developed targeting mercury ions, and whole-cell biosensors are among the most sensitive ones (Wang et al., 2013). Microbial biosensors can be easily embedded within portable devices, enabling rapid, on-site and low-cost monitoring (Gu M.B. et al., 2004, Lee et al., 2005, Stocker et al., 2003). Highly sensitive whole-cell biosensors were developed based on genetically reprogrammed cells for detecting several heavy metals, including arsenic, zinc, copper, cadmium and mercury (Selifonova et al., 1993; Van der Meer and Belkin, 2010; Wan et al., 2019). Cell engineering with fluorescent (FL) and bioluminescent (BL) reporter proteins, such as the green fluorescent protein and its variants and luciferases, under the regulation of specific regulatory pathways, such as mercury sensitive proteins (i.e. MerR) and their cognate regulated promoter (i.e. P_{merT}) provided new tools enabling the detection of mercury down to the femtomolar levels after 30 min of incubation with $HgCl_2$ using benchtop instrumentation (Lopreside et al., 2019b). However, the implementation of such powerful tools in portable analytical devices is not trivial and several attempts showed the difficulty of keeping cells viable and responsive not only during the analysis but also during storage and shipping. Different matrices and polymeric materials were explored to entrap microbial cells. The ideal material should have defined properties in terms of biocompatibility, absence of toxicity, ability to enable diffusion of sample and substrates, biodegradability, mechanical stability, and transparency for optical detection (Bae et al., 2020; Lobsiger et al., 2019; Lopreside et al., 2019b; Shemer et al., 2021; Jung et al., 2014). The well-established lyophilization method provided unbeatable results in terms of long-term stability. However lyophilized cells are not ready-to-use reagents, they must be “awakened” before use with incubation in liquid medium at a defined temperature for a given period of time (Bergua

et al., 2021). Instead, the ideal biosensor should be a stable all-in-one device embedding cells that are viable and responsive at use without prior treatments.

Other (bio)sensors were developed for the detection of Hg^{2+} exploiting, among others, aptamer and oligonucleotide-based strategies and different detection techniques such as electrochemical, FL and colorimetric ones (Şahin et al., 2020; Zhong et al., 2020). Besides aptamers, enzymes, such as β-galactosidase (β-gal), were also successfully integrated into paper sensors to detect irreversible inhibitors such as mercury and other heavy metals (Hossain and Brennan, 2011). Despite diverse prototypes for on-site analyses have been proposed, low-cost devices having the required sensitivity and robustness and able to analyze complex environmental matrices have not yet reached the market.

We aim to address the main issues that impede a true market penetration of current biosensors, such as lack of robustness and insufficient sensitivity, by developing an orthogonal biosensor providing the detection of mercury (II) via two different biorecognition elements, a BL mercury sensitive *Escherichia coli* bioreporter and an immobilized enzyme, β-gal, with BL and colorimetric detection, respectively. In addition, the inclusion of a BL strain, *Aliivibrio fischeri*, provides an internal toxicity control to correct the analytical signal, thus enabling the analysis of complex matrices. Both sensory elements and substrates necessary for the BL and colorimetric detection have been integrated into a paper sensor to provide an all-in-one disposable cartridge and a reusable 3D-printed case for smartphone signal acquisition (Figure 1).

[Figure 1 preferred position]

EXPERIMENTAL SECTION

Strains, chemicals and reagents

β-gal from *E. coli* (G6008-1KU), chlorophenol red-β-D-galactopyranoside (CPRG) substrate and all reagents required for colorimetric reaction were from Sigma-Aldrich (St. Louis, MO). *E. coli* TOP10 *J23109-merR-PmerT-NanoLuc* bacterial strain for mercury detection via NanoLuc luciferase expression has been obtained by PCR and Gibson Assembly (Lopreside et al., 2019b). Naturally bioluminescent bacteria *A. fischeri* were kindly gifted from Prof. Stefano Girotti (Camanzi et al., 2011).

Lysogeny broth (LB) medium and all reagents required for bacterial cell cultures were from Sigma-Aldrich (St. Louis, MO). Cryoprotectant R18 medium was prepared with 7.5 g/L tryptone, 100 g/L sucrose, 50 g/L bovine serum albumin (BSA) in ddH_2O.). B-PER lysing buffer for bacterial cell lysing was from Thermo Fisher Scientific (Waltham, MA, USA). Furimazine from NanoGlo Luciferase Assay System was from Promega (Madison, WI, USA).

Design of disposable sensing paper and 3D-printing of smartphone-based device

Whatman 1 CHR cellulose chromatography paper from GE Healthcare (Chicago, IL, USA) was used as support for the paper-based analytical device. A modular biosensor pattern was designed using PowerPoint (Microsoft, Redmond, WA, USA) and printed onto the Whatman 1 CHR chromatography paper using a Phaser 8400 office wax printer (Xerox, Norwalk, CT, USA). After printing, the waxed pattern was cured for 1 min at 100 °C to allow wax to diffuse in the paper thickness to create the hydrophobic areas (Montali et al., 2020). The paper-based disposable cartridge consisted of 12 circular hydrophilic “wells” (diameter 5 mm), named “CTR” (control well) and “T” (sample well), surrounded by hydrophobic areas (Figure 2A). A central bigger well (8 mm diameter) connected with each sample well (5 mm diameter) by tree channels (15 mm of length) was designed for single step sample addition. Two separate modules containing chromogenic and BL substrates, defined substrate-papers, were also designed overlapping the three-leaf sensing paper for independent substrate addition (Figure

2B). Adaptor and dark box for signal acquisition via smartphone were designed with the online 3D modeling program Tinkercad and printed with a desktop 3D printer Makerbot Replicator 2X. Black thermoplastic polymer acrylonitrile butadiene styrene (ABS) (FormFutura, Nijmegen, NL) at 300 µm layer resolution was used with 30% infill. A dark box (65 x 65 mm, 60 mm high) with smartphone adaptor (80 x 85 mm, 20 mm high) was designed with a front-side port (40 x 40 mm, 8 mm high) for cartridge integration. A reusable holder for the sensing paper was also designed (composed of 3 squares joined together, each one 40 x 40 mm and 8 mm high) with two subunits that can be held together by six N52 grade neodymium magnets (diameter 6 mm, thickness 2 mm) to assemble sample-paper and substrate-paper for signal acquisition (Figure 2A).

Colorimetric β-galactosidase paper (β-gal paper)

β-gal (500 U/mL) stock solution was prepared in 2 mL of PBS 0.1 M pH 7.4, sealed under nitrogen flow and stored at +4°C. 400 mg of CPRG were solubilized in 10 mL of ddH_2O to obtain a 68.4 mM (10x) stock solution. CPRG stock solution was stored protected from light at -20°C. Different concentrations, from 0.12 to 4 U/mL of β-gal were tested for immobilization on paper. β-gal concentration was optimized on paper with the preliminary absorption of 2 µL of 6.84 mM CPRG, subsequent addition of 10 µL of ddH_2O or sample and the addition of 5 µL of β-gal. Two alternative methods were evaluated, i.e., adsorption and lyophilization, to integrate β-gal on paper. For lyophilization, a 5 µl-volume of β-gal (1 U/mL) was deposited on a 5 mm-diameter paper well with R18 medium (from 0 to 50 $\%_{v/v}$). Due to the low sample volume, lyophilization was performed without sample freezing step using a Christ Alpha 1-2LD Plus Lyophilizer (Martin Christ Gefriertrocknungsanlagen GmbH, Germany), for 3 h, 0.029 mbar, -60°C (Calabretta et al., 2020). The optimized protocol involves the addition of a 5 µl-volume of β-gal (1 U/mL) with 20$\%_{v/v}$ of R18 medium for each well of the sensing paper

and a lyophilization step at -60°C for 3h at 0.029 mbar. The β-gal paper was then sealed into plastic bag and stored at + 4°C until use.

Bioluminescent papers with mercury-responsive *E. coli* strain (*E. coli* mercury-sensitive paper) and *A. fischeri* viability strain (*A. fischeri* toxicity paper)

To prepare the *E. coli* mercury-sensitive paper, *E. coli* TOP10 J23109-*merR*-P_{merT}-*nanoLuc* bacterial strain was cultured at 37°C, with orbital shaking at 200 rpm, in LB medium (10 g/L peptone, 5 g/L NaCl, 5 g/L yeast extract) plus 50 µg/mL of kanamycin. *A. fischeri* strain was cultured at 19°C, with orbital shaking at 200 rpm, in LB medium with high salinity (10 g/L peptone, 30 g/L NaCl, 5 g/L yeast extract), w/o antibiotic selection. Cell cultures were then centrifuged, and different concentrations were tested for biosensors characterization and integration with paper-based device.

Different immobilization methods and supplements were tested, along with different bacterial cells concentrations. For both *A. fischeri* and *E. coli* strains a cell concentration ranging from $1.6x10^4$ to $1.6x10^7$ cells/well was tested with or without $10\%_{w/v}$ trehalose, $50\%_{v/v}$ R18 medium, or $10\%_{v/v}$ of milk. Cell lyophilization, cell adsorption and entrapment into calcium alginate ($1.5\%_{w/v}$) or agarose ($0.75\%_{w/v}$) film were also evaluated. The optimized protocol to integrate the cells in the cartridge included 20 µL of cell suspension (OD_{600} = 0.1 for *E. coli* and OD_{600} = 5.0 for *A. fischeri*) in LB medium plus agarose gel ($0.75\%_{w/v}$) and $10\%_{w/v}$ trehalose.

Substrate-papers (CPRG-paper and Furimazine-paper)

The substrates for the colorimetric and BL reactions, CPRG and Furimazine, were lyophilized on paper for the development of a biosensor integrating all reagents required for the reactions. Different volumes from 2 µL to 4 µL of CPRG (6.84 mM) and from 10 µL to 20 µL of Furimazine (1:1000 and 1:500 dilutions in ddH_2O or B-PER lysing buffer) were tested.

Cryoprotectant or cofactors such as R18 medium (from 0 to 50%$_{v/v}$) and B-PER lysing buffer (from 0 to 99%$_{v/v}$) were co-lyophilized to increase biosensors responsiveness and stability. Liquid-dry lyophilization was performed as described before. In optimized conditions, CPRG-paper and Furimazine-paper were obtained lyophilizing 2 µL of CPRG (6.84 mM) and 10 µL of BL substrate (Furimazine 1:500 from Promega stock solution and 98%$_{v/v}$ of B-PER lysing buffer).

Signal acquisition and data analysis

BL signal acquisitions were carried out with a OnePlus 6T smartphone (OnePlus, Shenzhen, China), equipped with a dual integrated camera (primary sensor: 16 MP Sony Exmor RS IMX 519, BSI CMOS 1/2.600 colour sensor with 1.22-µm pixels, f/1.7 aperture; secondary sensor: 20 MP Sony Exmor RS IMX 376K, BSI CMOS 1/2.800 colour sensor with 1.0-µm pixels, f/1.7 aperture). Images were acquired using the secondary 20 MP camera from a 55 mm distance (height of the designed dark-box). BL images were acquired with Pro mode, with a selected ISO of 1600 and an acquisition time of 30 sec. Reflectance of colorimetric biosensor was acquired in standard mode using the integrated smartphone flash and the black box. Quantitative analysis of both colorimetric and BL signals was performed with the open-source Image J software (v. 1.52s, National Institutes of Health, Bethesda, MD, USA). A circular region of interest (ROI) was defined in correspondence of the biosensor well and the reflectance (colorimetric signal) was evaluated by the RGB analysis over the ROI area, while the BL signal was evaluated by integrating the BL image intensity over the ROI area (since maximum BL emission is at about 460-480 nm, integration was performed by considering only the blue channel of the RGB image). Regarding data obtained from images of the colorimetric biosensor, RGB system was considered as a three-dimensional space, whose 3 axes (x, y and z) correspond respectively to the 3 primary colours (red, green and blue). The x-axis (red) was

considered constant since the CPRG colorimetric reaction varies from red-violet to yellow-orange, thus maintaining high and constant red colour values. The two-dimensional Euclidean distance between the points on the y-axis and the points on the z-axis was then calculated to determine the curves, i.e. the two-dimensional distance between the green colour and the blue colour (Li et al., 2018). The maximum two-dimensional Euclidean distance obtained between the green and the blue channels, corresponding to yellow colour and complete enzyme inhibition by mercury(II), was set as 100%. GraphPad Prism v.5 (GraphPad Software, LaJolla, USA) was used to fit the data of samples with unknown concentration for the Hg(II) dose–response curves with a four parameter non-linear regression curve. As concerns the mercury-sensitive strain, the limit of detection (LOD) was calculated as mean value of control sample (ddH_2O) plus three times the standard deviation. For the β-gal, LOD was calculated as mean value of the control sample (red colour) minus three times the standard deviation of the control sample.

[Figure 2 preferred position]

Orthogonal biosensor assay procedure

After evaluating the optimal conditions in terms of analytical performances and incubation times of each sensing element of the biosensor, a straightforward procedure for simultaneous orthogonal detection of mercury(II) in liquid samples with the three different sensing papers in a single cartridge was developed and optimized. Briefly, the three-leaf sensing paper is placed in the 3D printed holder and a 150 µL-volume of sample is added to the central well. By capillarity the sample flows through the wax printed channels reaching sample wells. A 20 µL-volume of distilled water is added to control wells. Incubation times of 15, 30 and 60 min at room temperature are required for β-gal paper, *A. fischeri* toxicity paper, and *E. coli* mercury-

sensitive paper, respectively. After 15-minutes of incubation, the CPRG-paper overlapped to the sensing paper and closed with a complementary 3D printed adaptor. After 10 min, the colorimetric image is acquired introducing the β-gal paper inside a dark-box to avoid external light noise and using a OnePlus 6T smartphone camera with automatic mode and flashlight on. After 30-min incubation, *A. fischeri* toxicity paper is inserted into the dark box and BL signal acquired using a OnePlus 6T smartphone camera in Pro mode, with 30 sec of integration time and ISO 1600. After 60 min of incubation the Furimazine-paper is placed on the *E. coli* mercury-sensitive paper and is magnetically closed. The BL image is then acquired introducing the *E. coli* mercury-sensitive paper inside the dark-box using the OnePlus 6T smartphone camera.

Real sample analysis, and characterization of sensor recovery and selectivity

As proof-of-concept of the applicability of the developed biosensor with real samples, water samples, including tap water and lake water were spiked with different concentrations of mercury, interferents and toxic chemicals. Biosensor responsiveness to complex samples at different pH was assessed with tap water samples spiked with $HgCl_2$ (0.25 and 1.00 µM) with pH ranging from 2.5 to 7.5. Toxic samples were simulated with different concentrations of DMSO (from 0.50 to 50%$_{v/v}$) and fixed concentrations of mercury (0.50 µM and 0.25 µM). To evaluate the specificity of the biosensors, potential interferents like $CaCl_2$, $CdCl_2$, $NiCl_2$, AgCl and $MgCl_2$ were evaluated using the optimized procedure.

Recovery studies were performed using the optimized procedure and water samples spiked with mercury (from $5.00x10^{-3}$ to 1.00 µM) and DMSO (from 0.25 to 50%$_{v/v}$). Recoveries were calculated by applying a signal correction for *E. coli* mercury-sensitive paper. The corrected BL value was obtained by multiplying the raw value, obtained from the sensing paper, by a correction factor, calculated as the ratio, for each tested sample, between the BL signal of *A.*

fischeri-toxicity paper incubated with ddH_2O (control) and the signal of *A. fischeri* toxicity-paper incubated with the sample.

All experiments were performed in triplicate and repeated at least three times.

Biosensor stability evaluation

The stability for *E. coli* and *A. fischeri* immobilized in agarose ($0.75_{\%w/v}$) with $10\%_{w/v}$ of trehalose and lyophilized β-gal (1 U/mL) with $20\%_{v/v}$ of R18 medium was assessed by keeping the sensing papers in sealed plastic bags for several weeks at + 4 °C. After 24, 48, 72, 96 hours, 1 week, 2 weeks and 1 month, the plastic bags were opened to perform the assay at room temperature (25°C), as described previously. To assess substrate stability, the substrate-papers containing the lyophilized substrate (CPRG and Furimazine) were stored in sealed plastic bags at + 4°C and tested after 24, 48, 72, 96 hours, 1 week and 2 weeks as described before.

RESULTS AND DISCUSSION

Design of disposable paper-based cartridge and 3D-printing of the integrated smartphone-based device

We developed a low-cost biosensor for orthogonal detection of mercury(II) integrating three different biorecognition elements on a disposable three-leaf paper: i) a mercury-specific BL *E. coli* bioreporter strain expressing the mercury receptor MerR under the regulation of a constitutive promoter (J23109) and NanoLuc luciferase under the regulation of promoter P_{merT}, ii) a purified β-gal enzyme which is irreversibly inhibited by mercury and other metal ions reacting on the sulfhydryl group of cysteine, and iii) a *A. fischeri* BL strain for sample toxicity evaluation and analytical signal correction (Figure 1). The mercury-specific BL *E. coli* bioreporter strain expresses the mercury receptor MerR under the regulation of a constitutive promoter (J23109), and mercury interacts with this receptor constitutively produced by the *E.*

coli strain. In the presence of increasing concentrations of mercury(II), The mercury receptor MerR derepresses its cognate promoter P_{merT} leading to the expression of the BL NanoLuc protein.

The purified β-gal enzyme is irreversibly inhibited by mercury and other metal ions reacting on the sulfhydryl group of cysteine in the active site of the enzyme. In the presence of increasing concentrations of mercury(II) the enzymatic function is inhibited and the colour changes from red-purple to yellow colour. The BL control signal emitted by the *A. fischeri* strain decreases due to sample toxicity. Paper was chosen as support to integrate the three biosensing elements since it is sustainable, allows passive transport of liquid and shows high biocompatibility with several biomolecules and living cells as well. Few examples report the integration of whole-cell biosensors into paper (Guo et al., 2020; Liu et al., 2018; Ma et al., 2020) and, to the best of our knowledge, the present biosensor represents the first attempt to integrate living cells, enzymes and their corresponding substrates, in the same device to create a stable biosensor providing an easy and rapid assay procedure. The first challenge was to address both cell and enzyme immobilization in the same paper support to enable storage of the device without activity loss. We decided to lyophilize the enzyme and entrap the cells in a hydrogel to combine advantages of the two approaches and to obtain a ready-to-use sensing paper that does not require any additional step for "awakening" the cells and that can be stored and shipped without a strict cold chain. As concerns the detection, we combined BL detection required for the two whole-cell biosensors, the mercury specific strain and the viability control strain, with colorimetric detection of β-gal obtained with the chromogenic substrate CPRG. A low-cost 3D-printed case was fabricated to enable standardized rapid and robust smartphone detection for all the three biosensing reactions.

Colorimetric β-galactosidase paper

Preliminary experiments involving different concentrations and volumes of CPRG and β-gal were performed to identify the suitable combination providing the highest sensitivity of the paper sensor. A colour change from yellowish-orange to red-purple was observed at increasing enzyme concentrations, leading to a decreased bidimensional distance between the green and blue channels of the RGB system (Figure S1). The lowest concentration tested (0.12 U/mL) showed the maximum variation (48%) from the control. The highest concentration tested (4 U/mL) showed an opposite maximum variation from the control (155%) due to a negative Euclidean distance (purple colour). No difference in reflectance was observed between the highest enzymatic concentrations (2 and 4 U/mL) in that the ratio of the Euclidean bi-dimensional distance between these two concentrations was 1.16. Regarding response time, low enzyme concentrations required more time for colour change (up to 10 min to obtain a red colour, instead of 5 min for 1 U/mL β-gal) while higher enzyme concentrations (2 and 4 U/mL) result in a rapid colour change (from yellow to red colour) and a saturated signal that leads to a negative distance between green and blue channel of RGB system. Accordingly, a β-gal concentration of 1 U/mL and a CPRG concentration of 6.84 mM, providing a positive Euclidean bi-dimensional distance close to zero and showing the maximum variation from the control of 95%, were selected.

Different lyophilization procedures and addition of cryoprotectants were evaluated. The addition of R18 at concentrations higher or equal than 10 $\%_{v/v}$ caused the preservation of β-gal enzymatic function and a colour change from yellow to red comparable to the one obtained before the freeze-drying process. Comparing the two-dimensional Euclidean distance between the green and blue channel obtained before and after freeze-drying, a 1.18 ratio was obtained with the lyophilization of a 5 µL volume of 1 U/mL β-gal with 20 $\%_{v/v}$ of R18 medium. Higher concentrations of R18 medium resulted in a spurious colour change (dark red), (Figure S1).

Therefore, the optimal lyophilization method was obtained with 5 µL of 1 U/mL β-gal with 20 $\%_{v/v}$ of R18 medium for each well of the sensing paper.

Bioluminescent *E. coli* mercury-sensitive paper and *A. fischeri* toxicity paper

To develop a ready-to-use sensor integrating the two bacterial reporters with long stability we first tested lyophilization of bacterial cells with different cryoprotectants and conditions. The use of R18 medium and trehalose ($10\%_{w/v}$) provided a significant improvement of cell viability after storage at + 4 °C, up to 4 weeks, with an increased BL signal of 3.6 and 2.2 folds higher than that obtained with LB medium. Nevertheless, a minimum of 16 h of incubation at room temperature with liquid medium was required to reactivate cell metabolism and use the cells for biosensing. Accordingly, alternative approaches were investigated to develop a ready-to-use biosensor with active bacterial cells on paper. Agarose and calcium alginate were combined with different cell concentrations to improve cell viability and to obtain a BL signal detectable with smartphone-integrated CMOS. A 20 µL-volume of cell suspension with an OD_{600} of 0.1 for *E. coli* and OD_{600} 5.0 for *A. fischeri* (corresponding to $1.6x10^6$ and $8x10^7$ cells, respectively) in LB medium with $10\%_{w/v}$ trehalose or $7.5\%_{w/v}$ of agarose were deposited on paper. A complete loss of BL signal was observed after bacterial dehydration on paper without hydrogel (Figure S1); while a BL signal was produced by cells entrapped on hydrogel, corresponding to 123% of the BL signal obtained with the liquid cell culture. The addition of milk ($10\%_{v/v}$) in hydrogel caused a 1.4-fold signal increase when compared to the control (same cell concentration in LB medium). No change or signal increase was caused by trehalose addition (Figure S1). No significant differences on cell viability were obtained with entrapment of cells into alginate, which provided a BL signal only 1.2 fold higher than obtained with agarose immobilization. Instead, cells entrapped in sodium alginate did not attach to the paper support and after drying almost complete detachment of cells was observed. Our results support those

reported by Gu Z. et al., who demonstrated that agarose binds to filter paper fibers and that hydrogel coated region presents a relatively "slow" absorption of liquid, which may facilitate the interaction between the immobilized bacteria and the sample (Gu Z. et al., 2011).

Chromogenic and bioluminescent substrate-papers

Two substrate papers have been designed complementary to the three-leaf sensing paper to obtain an all-in-one and liquid-free biosensor. A 2 µL-volume of CPRG (6.84 mM) and a 10 µL-volume of Furimazine were lyophilized on paper. CPRG was lyophilized without adding cryoprotectant because addition of $25\%_{v/v}$ and $50\%_{v/v}$ of R18 medium increased the Euclidean two-dimensional distance between the RGB signal in the green channel and the signal in the blue channel of 2.25 times and 6.64 times, respectively. The increase of the Euclidean distance corresponded to a lower reactivity of the substrate which did not allow the colorimetric reaction to proceed. Lyophilized CPRG, without cryoprotectant, is stable for a long time when stored at + 4 °C sealed in plastic bags with a 100% stability up to 4 weeks post lyophilization. In addition, Furimazine substrate, required for the NanoLuc-catalyzed BL reaction, was lyophilized in the presence of a lysing buffer to obtain a stable reagent for the *E. coli* mercury-sensitive paper. Following 4 weeks storage at + 4 °C sealed in plastic bags a BL signal corresponding to 98% of the signal obtained at day 0 was obtained. A high stability of Furimazine was also proven by Hall et al. who reported no loss in activity after 11 months at ambient temperature (Hall et al., 2021).

Analytical performance of the three-leaf bioluminescent/colorimetric paper biosensor

The analytical performance of the smartphone-based three-leaf biosensor was assessed using standard solutions and simulated toxic samples (see paragraph "Three-leaf biosensor's characterization", SI). The kinetics of the colorimetric and BL signals were obtained by

incubating, up to two hours, each well of three-leaf biosensor with 20 µL of 1 µM $HgCl_2$ as model analyte for induction and 25%$_{v/v}$ DMSO as model toxic compound (Fig 4A). The β-gal paper produced a signal with a kinetic with a plateau reached after 15 min of incubation and a signal stable for at least 120 min, due to the irreversible inhibition of the enzyme. Accordingly, the incubation time for the colorimetric detection of mercury(II) was set at 15 min. Moreover, to standardize the measurement an optimal acquisition window from 10 to 13 min, after CPRG addition, was identified with stable reflectance signal (Figures S2-S4). The *E. coli* mercury-sensitive paper produced an emission kinetic with a maximum BL signal over control after 60 min. This behavior is consistent with the time required to express the NanoLuc reporter protein (Lopreside et al., 2019b). Therefore, the incubation time for mercury(II) detection via BL *E. coli* sensor strain was set at 60 min.

A decrease of the BL signal for *A. fischeri*-paper was observed over time due to DMSO toxicity. The 100% signal was set for *A. fischeri* incubated with ddH_2O (control) and a 43% of signal reduction was observed after 30 min of incubation. Since the curve reached a stable BL signal after 30 min, this incubation time was selected for *A. fischeri* paper.

Incubation times of 15, 30 and 60 min were selected for β-gal paper, *A. fischeri* toxicity paper and *E. coli* mercury-sensitive paper, respectively.

Figure 3B shows the dose-response curves of *A. fischeri* toxicity paper and *E. coli* mercury-sensitive paper incubated with samples of varying $HgCl_2$ concentrations (from $5.00x10^{-4}$ to 1.00 µM). *A. fischeri* exhibited mercury toxicity at $HgCl_2$ concentrations higher than 0.25 µM. This toxicity assessment was necessary to correct the BL signal obtained with the *E. coli* mercury-sensitive paper and avoid underestimation due to sample toxicity or overestimations in the presence of matrix effects that improve cell metabolism. Signal correction according to cell viability and metabolism is required to obtain robust results from whole-cell biosensors (Mirasoli et al., 2002), especially for the analysis of complex matrices, however few examples

of devices integrating analyte-specific bioreporters and general toxicity strains have been reported (Cevenini et al., 2018; Lopreside et al., 2019a; Roda et al., 2011).

By correcting the BL signal obtained from the *E. coli* mercury-sensitive paper with the *A. fischeri* toxicity paper signal, a dose response curve was obtained showing a LOD of $2.87x10^{-3} \pm 3.45x10^{-4}$ µM for $HgCl_2$. This LOD corresponds to 0.58 ± 0.07 ppb for Hg^{2+}, thus allowing the measurements of the maximum allowed concentration of mercury(II) in drinking water of 2 ppb (10 nM) and 6 ppb fixed by U.S. Environmental Protection Agency (EPA) and the World Health Organization (WHO), respectively (US EPA, 2009; WHO, 2011) .

The corrected dose-response curve obtained with *E. coli* mercury-sensitive paper was compared with the dose response curve obtained with the β-gal paper treated with samples of varying concentrations of $HgCl_2$ (Figure 3). The LOD obtained with the β-gal paper was $8.50x10^{-2} \pm 0.01$µM, corresponding to 17.0 ± 2.20 ppb for Hg^{2+}.

[Figure 3 preferred position]

Comparing the corrected signal of the *E. coli* mercury-sensitive paper with the β-gal paper, bacterial cells showed a lower LOD, albeit with a longer incubation time, 60 min *vs* 15 min. Both LODs are in the same order of magnitude obtained by others previously reported (Guo et al., 2020; Sajed et al., 2019) but faster response time (Figure 4).

For example, Guo et al. developed a whole-cell microbial biosensor based on FL reporter gene with a LOD of 1 mg/kg for total inorganic mercury pollutants in cosmetics with 6 h incubation time (Guo et al., 2020). In a pioneering work, three microbial bioreporters were developed to detect Hg(II) in waters in the 0.50 - 1000 nM range (0.10 to 200 ppb), thus similar to the analytical performance of the *E. coli* mercury-sensitive paper, albeit with benchtop instrumentation and necessity of growing bacterial cultures (Selifonova et al., 1993). Notably,

Wan et al., combining different cascaded amplifying circuits in a FL whole-cell sensor array, were able to detect mercury down to 0.01 ppb, with 6 h incubation and benchtop laboratory instrumentation (Wan et al., 2019).

[Figure 4 preferred position]

Biosensor analytical performance with simulated complex samples

Simulated complex samples with mixed toxic activity and mercury contamination were analysed with the three-leaf biosensor (Figure 5 A, B). Both colorimetric and BL biosensors showed a signal decrease directly proportional to the increased toxicity. For example, in the presence of 0.50 µM Hg^{2+} at pH 4.6 and pH 7.0, a similar signal decrease of 16% and 17% were obtained, for the *E. coli*-mercury-sensitive paper and β-gal paper, respectively. For the same concentration, the signal decrease obtained with the *A. fischeri* toxicity paper was 11%, confirming its suitability for signal correction. We next analysed solutions with more acidic pH (pH 3.0, Figure 5A, Figure 6) that caused an almost complete cell death of *A. fischeri* bacteria (BL signal corresponding to 4% of the control BL signal,), supporting the necessity to perform a signal correction to avoid artefact results. In fact, in the presence of 0.50 µM of Hg^{2+} at pH 3.0, the *E. coli* mercury-sensitive paper showed a response decrease of 85%. On the other hand, the β-gal paper, on the basis of β-galactosidase inhibition in the presence of mercury, showed a false positive response. An enzyme inhibition of 90% was detected for acidic water (pH 3.0) without mercury, compared to 88% of enzymatic inhibition in the presence of 1.00 mM of Hg^{2+} (Figure 5A). *A. fischeri*-paper was able to respond to different pH changes from 2.5 to 5.5. BL signal decreases of 8% and 96% were observed at pH 5.3 and pH 2.7, respectively. Acute cytotoxicity was found starting at pH 4.0 with loss of 60% of cell viability.

Therefore, to properly correct the analytical signal, we defined a viability threshold corresponding to 20% of cell toxicity, obtained at pH 4.5.

DMSO was used as model toxic analyte to simulate general sample toxicity and to investigate the suitability of analytical signal correction according to the control signal obtained with the *A. fischeri* toxicity paper. A fixed concentration of Hg^{2+} (0.50 µM) was mixed with varying DMSO concentrations before biosensor response was evaluated. A signal decrease was observed with 0.50 µM $Hg^{2+}$and DMSO concentrations higher than 5%$_{v/v}$. A 5%$_{v/v}$ DMSO concentration caused *A. fischeri* cytotoxicity of 13% and a signal decrease of 41% and 15% for *E. coli* mercury-sensitive paper and β-gal paper, respectively (Figure 5). With such high level of toxicity signal correction therefore could not be applied.

A mercury(II) concentration of 0.49 ± 0.02 µM was calculated by applying the correction of analytical signal for a sample containing DMSO 0.5%$_{v/v}$ and 0.50 µM of Hg^{2+} while without the correction a concentration of mercury(II) of 0.45 ± 0.02 µM was obtained, demonstrating the usefulness of the signal correction for the analysis of toxic samples. The calculated recovery was 98%, while a 90% recovery was obtained without applying the signal correction. However, for samples causing excessive cell death, the correction did not allow to obtain accurate results. For example, the recovery for a sample with 0.50 µM of Hg^{2+} and DMSO 25% $_{v/v}$ was 81 % with signal correction (Table S1). In this case, a biosensor viability threshold was set for samples having cytotoxicity ≥ 20% (obtained with DMSO confrontations ≥ 10%$_{v/v}$). DMSO 10%$_{v/v}$ caused a signal decrease of 55% for the *E. coli*-paper and 44% for the β-gal paper.

[Figure 5 preferred position]

Specificity studies

The three-leaf biosensor specificity was evaluated with various interferents measured at a concentration of 1.00 µM (Figure 5,6). Control well signals were normalized as 100% of signal for all the sensing papers. In the presence of 1 mM Hg^{2+}, used as the positive control, an induction of 400% for *E. coli* mercury-sensitive paper and an inhibition of 88% for β-gal paper was reached. No interference was detected for both sensing papers in the presence of highly concentrated Mg^{2+} (101% and 104% for the *E. coli* mercury sensitive paper and the β-gal paper). A different behavior was observed in the presence of Ca^{2+}, no induction was reported with the *E. coli* mercury-sensitive paper, while a 43% inhibition was reported with the β-gal paper. A similar behavior was found with Cd^{2+} which caused a 44% inhibition of β-gal while no signal increase was reported for the *E. coli* mercury-sensitive paper. In contrast, 1.00 µM Ni^{2+} showed no inhibition of β-gal activity, in agreement with previous reports (Hossain and Brennan, 2011), and a low induction of *E. coli* mercury-sensitive paper (143%). At the same concentration, Ag^{+} showed a low level of induction (121%) for *E. coli* mercury-sensitive paper and an almost complete inhibition (91%) for β-GA β-gal paper. The inhibition of Ag^{+} and Cd^{2+} is consistent with previous reports (Hossain and Brennan, 2011) and, while Ag^{+} is not a commonly encountered water contaminant, the presence of Cd^{2+} in drinking water and rivers, even at low concentrations, is toxic to all living organisms, with a maximum limit in groundwater of 3.00 µg/L (WHO, 2004). Excluding mercury, none of the metals at the tested concentration (1.00 µM) showed significant cytotoxic effects; the highest cytotoxicity effects were obtained with Cd^{2+} with a 6% of signal decrease (Figure 6).

Recovery studies

Recovery studies were performed to demonstrate the applicability of the three-leaf paper biosensor for mercury(II) detection in water samples and in simulated toxic samples. Water samples were spiked with different mercury concentrations in the presence of a toxic compound (DMSO). In the absence of toxicity (0%$_{v/v}$ DMSO) both the colorimetric and BL sensing papers provided a good recovery for all the tested concentrations (Table S1). With 10%$_{v/v}$ and 25%$_{v/v}$ DMSO concentrations a toxicity of 20% and 50% was observed with the *A. fischeri* toxicity paper and a different behaviour was observed for the *E. coli* mercury-sensitive paper and the β-gal paper. In the presence of 2.5%$_{v/v}$ DMSO and 0.25 µM of Hg^{2+} (toxicity lower than 10%) a recovery of 112% was obtained by applying the *A. fischeri* signal correction. In contrast, at higher toxicity, such as with 25% DMSO a complete inhibition of β-gal was observed. This inhibition, without the inclusion of a toxicity sensor paper in the same device, could cause an erroneous interpretation with a false positive output. Therefore, this approach could be extended to all biosensors relying on living cells or enzymes to avoid artefact results.

[Figure 6 preferred position]

Biosensor's stability evaluation

The reproducibility of the immobilization procedures was evaluated using the constitutive BL signal of *A. fischeri* immobilized according to the procedure described in the experimental section with agarose (7.5%$_{w/v}$) and trehalose (10% $_{w/v}$). We obtained, by immobilizing approximately $8x10^7$ cells/well an average BL signal of $1.35x10^6$ RLU and a CV% of 18% (30 wells). An increased BL signal (1.2 fold higher) of freshly immobilized bacteria was observed for bacteria immobilized in calcium alginate compared to those immobilized into agarose gel. However no significant signal changes were reported after 7 days storage for the two immobilization methods. Instead, a significant increase of BL signal was observed for bacteria

immobilized in either agarose or calcium alginate supplemented with trehalose (10% $_{w/v}$) and milk (10% $_{v/v}$). The addition of trehalose (10% $_{w/v}$) resulted in BL signal 2.7 and 2.9 fold higher (at time 0) for bacteria immobilized in calcium alginate and in agarose, respectively; the addition of milk caused 2.9 and 2.2 fold increase of BL signal for calcium alginate and agarose, respectively. Unexpectedly, no significant viability improvement was observed after storage with both supplements. The *A. fischeri* toxicity paper supplemented with agarose 0.75%$_{w/v}$ remained responsive for 7 days, at 4 °C, sealed in plastic bag, with a maximum signal decrease of 25% and CV% of 19%. As for the *A. fischeri* paper the same stability was evaluated for the *E. coli* mercury-sensitive paper.

Concerning the β-gal paper, the stability was evaluated up to 2 months by lyophilizing 5 µL of 1 U/mL β-galactosidase with 20 %$_{v/v}$ of R18 medium directly on the paper. The β-gal paper was sealed in plastic bags and stored at 4 °C. The enzymatic activity of the β-gal paper after 24, 48, 72 h and 1 week was 100%, 103%, 98% and 106% respectively. After 4 weeks the enzymatic activity was 94% while after 5 weeks a 45% decrease in the enzymatic activity was observed. After 2 months the enzymatic activity was equal to 24% of the initial one.

CONCLUSIONS

We developed a new biosensor integrating two different biorecognition elements, responding to the same analyte, mercury(II), and a toxicity control in the same device to improve the robustness and accuracy of mercury(II) detection in complex samples, such as samples with a certain level of toxicity.

The integration of microbial biosensors and enzymes combined with exploitation of different optical detection modes, i.e., BL and colorimetric detection, allowed us to develop a biosensor with higher robustness and did not affect neither the complexity of the biosensor design nor the workflow of assay procedure. In fact, the inclusion of β-gal, having a response time within

15 min, provides a very quick response about presence of potential health threats well in advance to the light signal emitted by the mercury-sensitive whole-cell biosensor, which requires 1 hour of incubation with the sample. Moreover, the lack of specificity of β-gal, which is certainly a drawback in standard laboratory-based analytical techniques, turns out to be useful to provide a first level "warning" about the possible presence of other toxic heavy metals such as cadmium. In addition, thanks to the inclusion of a pre-made substrate-paper containing chromogenic and BL substrates the device does not require additional steps such as substrate addition, simplifying the assay procedure and enabling its use by non-skilled personnel. Owing to its analytical performance we envisage possible applications of the developed biosensor to monitor drinking water, surface waters or industrial waters as a rapid and low-cost screening tool in the field before more accurate and expensive analyses are performed.

ACKNOWLEDGEMENTS

Funding: this research was funded in part by the NATO Science For Peace And Security Programme under grant no. 985042 and FEDKITO project funded by MIUR and Prima (Partnership for Research and Innovation in the Mediterranean Area). Baojun Wang acknowledges support by the UK Research and Innovation Future Leaders Fellowship [MR/S018875/1] and US Office of Naval Research Global grant [N62909-20-1-2036].

REFERENCES

Bae, J.W., Seo, H.B., Belkin, S., Gu, M.B., 2020. Anal. Bioanal. Chem. 412, 3373-3381.

Bergua, J. F., Álvarez-Diduk, R., Hu, L., Hassan, A. H., Merkoçi, A., 2021. J. Hazard. Mat. 406, 124434.

Calabretta, M.M., Álvarez-Diduk, R., Michelini, E., Roda, A., Merkoçi, A., 2020. Biosens. Bioelectron. 150, 111902.

Calabretta, M.M., Montali, L., Lopreside, A., Fragapane, F., Iacoangeli, F., Roda, A., Bocci, V., D'Elia, M., Michelini, E., 2021. Anal. Chem., 93, 20, 7388–7393.

Camanzi, L., Bolelli, L., Maiolini, E., Girotti, S., Matteuzzi, D., 2011. Environ. Toxicol. Chem. 30, 801-805.

Cevenini, L., Lopreside, A., Calabretta, M.M., D'Elia, M., Simoni, P., Michelini, E., Roda, A., 2018. Anal. Bioanal. Chem. 410, 1237-1246.

EFSA Scientific Committee, 2015. EFSA journal, 13(1), 3982.

European Commission, 2012. Report from the Commission to the European Parliament and the Council on the Implementation of the Water Framework Directive (2000/60/EC) River Basin Management Plans.

European Environment Agency, 2018. Mercury in Europe's environment: A priority for European and global action. Publications Office of the European Union.

Gu, M. B., Mitchell, R. J., Kim, B. C., 2004. Biomanufact. 269-305.

Gu, Z., Zhao, M., Sheng, Y., Bentolila, L. A., Tang, Y., 2011. Anal. Chem., 83, 2324-2329.

Guo, M., Wang, J., Du, R., Liu, Y., Chi, J., He, X., Huang, K., Luo, Y., Xu, W., 2020. Biosens. Bioelectron., 150, 111899.

Hall, M.P., Kincaid, V.A., Jost, E.A., Smith, T.P., Hurst, R., Forsyth, S.K., Fitzgerald, C., Ressler, V.T., Zimmermann, K., Lazar, D., Wood, M.G., Wood, K.V., Kirkland, T.A., Encell, L.P., Machleidt, T., Dart, M.L., 2021. Anal. Chem. 93, 5177-5184.

Hossain, S.M., Brennan, J.D., 2011. Anal Chem. 83, 8772-8.

Jung, I., Seo, H.B., Lee, J.E., Kim, B.C., Gu, M.B., 2014. Analyst. 139, 4696-701.

Lee, J. H., Mitchell, R. J., Kim, B. C., Cullen, D. C., Gu, M. B., 2005. Biosens. Bioelectron. 21(3), 500-507.

Lemm, J.U., Venohr, M., Globevnik, L., Stefanidis, K., Panagopoulos, Y., van Gils, J., Posthuma, L., Kristensen, P., Feld, C.K., Mahnkopf, J., Hering, D., Birk, S., 2021. Glob. Chang. Biol. 27(9), 1962-1975.

Leopold, K., Foulkes, M., Worsfold, P. Anal Chim Acta. 2010 ;663(2) 127-38.

Li, L., Zhang, L., Zhao, Y., Chen, Z., 2018. Microchim. Acta. 185, 235.

Liu, J., Morales-Narváez, E., Orozco, J., Vicent, T., Zhong, G., Merkoçi, A., 2018. Nano Res. 11(1), 114-125.

Lobsiger, N., Venetz, J.E., Gregorini, M., Christen, M., Christen, B., Stark, W.J., 2019. Biosens. Bioelectron. 146, 111710.

Lopreside, A., Calabretta, M.M., Montali, L., Ferri, M., Tassoni, A., Branchini, B. R., Southworth, T., D'Elia, M., Roda, A., Michelini, E., 2019a. Anal. Bioanal. Chem. 411(19), 4937-4949.

Lopreside, A., Wan, X., Michelini, E., Roda, A., Wang, B., 2019b. Anal. Chem. 91, 15284-15292.

Ma, Z., Liu, J., Sallach, J. B., Hu, X., Gao, Y., 2020. Biosens. Bioelectron. 168, 112528.

Minamata Convention on mercury, 2020 Progress Report 2020 https://mercuryconvention.org/Portals/11/documents/Minamata-Progress-report-2020.pdf

Mirasoli, M., Feliciano, J., Michelini, E., Daunert, S., Roda, A., 2002. Anal. Chem. 74, 5948-53.

Montali, L., Calabretta, M.M., Lopreside, A., D'Elia, M., Guardigli, M., Michelini, E., 2020. Biosens. Bioelectron., 162, 112232.

Roda, A., Roda, B., Cevenini, L., Michelini, E., Mezzanotte, L., Reschiglian, P., Hakkila, K., Virta, M., 2011. Anal. Bioanal. Chem. 401, 201-211.

Şahin, S., Caglayan, M.O., Üstündağ, Z., 2020. Talanta. 220, 121437.

Sajed, S., Arefi, F., Kolahdouz, M., Sadeghi, M.A., 2019. Sensor. Actuat. B-Chem. 298, 126942.

Selifonova, O., Burlage, R., Barkay, T., 1993. Appl. Environ. Microbiol. 59, 3083-90.

Shemer, B., Shpigel, E., Hazan, C., Kabessa, Y., Agranat, A.J., Belkin, S., 2020. Microb. Biotechnol. 14, 251-261.

Stocker, J., Balluch, D., Gsell, M., Harms, H., Feliciano, J., Daunert, S., Malik, K.A., Van der Meer, J.R., 2003. Environ. Sci. Technol. 37, 4743-4750.

Van der Meer, J.R., Belkin, S., 2010. Nat. Rev. Microbiol. 8, 511-22.

U.S. EPA. National Primary Drinking Water Regulations. 2009. https://www.epa.gov/ground-water-and-drinking-water/national-primary-drinking-water-regulations

Wan, X., Volpetti, F., Petrova, E., French, C., Maerkl, S.J., Wang, B., 2019. Nat. Chem. Biol. 15, 540-548.

Wang, B., Barahona, M., Buck, M., 2013. Biosens. Bioelectron. 40, 368-376.

WHO, 2004. Cadmium in drinking-water: background document for development of WHO guidelines for drinking-water quality. World Health Organization, Geneva.

WHO, 2011. Guidelines for Drinking Water Quality, 4th ed.; World Health Organization: Geneva, http://whqlibdoc.who.int/publications/2011/9789241548151_eng.pdf

Zhong, Y.Q., Ning, T.J., Cheng, L., Xiong, W., Wei, G.B., Liao, F.S., Ma, G.Q., Hong, N., Cui, H.F., Fan, H., 2021.Talanta. 23, 121709.

Figure legends

Figure 1. Schematic showing the design of the three-leaf biosensor. The paper sensor integrates two mercury-specific biorecognition elements, BL bacteria carrying NanoLuc luciferase induced by Hg^{2+} and β-gal enzyme irreversibly inhibited by Hg^{2+}, with a BL *A. fischeri* strain, used to correct the analytical signals according to sample toxicity. BL and colorimetric signals are measured with the smartphone camera. A 3D printed dark box protects the sensing papers from ambient light for BL detection and enables the use of smartphone-integrated flash for β-gal colorimetric detection.

Figure 2. 3D-printed device and user-friendly procedure for sample testing.

A) Components of the orthogonal biosensor device. Disposable paper cartridge including a three-leaf sensing paper, enabling analysis of test sample (T) and control (CTR) in duplicate, two substrate papers (S), containing either CPRG or BL substrate for separate analysis, magnetic reusable 3D-printed holder and dark box with smartphone adaptor. **B)** Step-by-step procedure for sample analysis.

Figure 3. Analytical performance and characterization of the three-leaf bioluminescent-colorimetric paper biosensor A) Biosensor's response over time with $HgCl_2$ (1 µM) for *E. coli* mercury-sensitive paper and β-gal paper, and DMSO-25%$_{v/v}$ for *A. fischeri* toxicity paper; **B)** Dose response curves of the *E. coli* mercury-sensitive paper (with/without signal correction) and *A. fischeri* toxicity paper with different concentrations of $HgCl_2$; **C)** Normalized dose response curves of *E. coli* mercury-sensitive paper (corrected curve) and β-gal paper with $HgCl_2$;

Figure 4. Pictures of the three-leaf bioluminescent- colorimetric paper biosensor. Pictures of sensing papers responding to samples with varying concentrations of Hg^{2+}: *A. fischeri* toxicity paper *(left), E. coli* mercury-sensitive paper (center) and β-gal paper (right).

Figure 5. Mercury(II) detection with the three-leaf biosensor, interference and selectivity studies. A) Biosensor response to simulated complex samples with Hg^{2+} and pH-induced cytotoxicity effect; **B)** Biosensor inhibition induced by increasing cytotoxicity effect of varying DMSO concentrations with Hg^{2+} 0.50 µM; **C)** Biosensor response to different interferents (1.00 µM).

Figure 6. Selectivity studies. A) Pictures of the three-leaf biosensor responses to different compounds and with different simulated complex samples; **B)** Images showing the results of the three-leaf biosensor for Hg^{2+} detection.

Supporting Information

Orthogonal paper biosensor for mercury (II) combining bioluminescence and colorimetric smartphone detection

Antonia Lopreside[1,2¥], Laura Montali[1,2¥], Baojun Wang[3], Annalisa Tassoni[4], Maura Ferri[4,5],Maria Maddalena Calabretta[*1,2] and Elisa Michelini[*1,2,3,4]

[1] Department of Chemistry "Giacomo Ciamician", University of Bologna, Via Selmi 2, 40126 Bologna, Italy

[2] Centro di Ricerca Biomedica Applicata (CRBA), Azienda Ospedaliero-Universitaria Policlinico S. Orsola-Malpighi, Bologna, Italy

[3] Centre for Synthetic and Systems Biology, School of Biological Sciences, University of Edinburgh, Edinburgh, United Kingdom

[4]Department of Biological, Geological and Environmental Sciences, University of Bologna, Via Irnerio 42, 40126 Bologna, Italy.5

[5]Department of Civil, Chemical, Environmental and Materials Engineering, University of Bologna, Bologna, Italy.

[6]Health Sciences and Technologies-Interdepartmental Center for Industrial Research (HST-ICIR), University of Bologna, via Tolara di Sopra 41/E 40064, Ozzano dell'Emilia, Bologna, Italy

[¥] These authors contributed equally.

* Corresponding authors: elisa.michelini8@unibo.it; maria.calabretta2@unibo.it

EXPERIMENTAL SECTION

Three-leaf biosensor's characterization

A preliminary optimization of the three different sensing papers was performed using paper cartridges with 3x7 wells (5 mm diameter) in order to optimize LOD, analytical performances and incubation times of each component of the three-leaf biosensor separately.

Biosensor responsiveness and analytical performance were first evaluated with different concentrations of $HgCl_2$ as model analyte, from $1.00x10^{-4}$ to 1.00 µM. Limit of detection (LOD), fold response, incubation times and kinetic measurements from 0 to 120 min of incubation (at room temperature) for the three sensing papers were performed to identify the suitable temporal window for signal acquisition. For β-gal paper optimization, preliminary studies were performed using a 2 µL-volume of 6.84 mM CPRG solution absorbed on paper incubated with 5 µL of 1.00 U/mL β-galactosidase and 20 µL of 1.00 µM $HgCl_2$ solution. The β-gal paper was also tested with different $HgCl_2$ volumes from 5 to 25 µL to identify the optimal reaction conditions. The incubation time of $HgCl_2$ with β-gal paper was optimized by adding a 20 µL-volume of a 1.00 µM $HgCl_2$ solution on the well with β-galactosidase lyophilized and incubating up to 120 min. After incubation, a 2 µL-volume of 6.84 mM CPRG solution was added. As regards the final optimization of the β-gal paper, 20 µ L of $HgCl_2$ (from $1.00x10^{-4}$ to 1.00 µM) were added on the well with the lyophilized β-galactosidase and left to incubate for 15 min at room temperature (25°C). After incubation, the substrate paper was positioned, and the colorimetric image acquired with the smartphone camera. To choose the optimal time window for the colorimetric image acquisition, kinetics of colorimetric signal obtained with CPRG substrate were evaluated, taking images every minute for 20 min. As concerns *E. coli* mercury-sensitive paper, different volumes (from 5 to 25 µL) of sample (1.00 µM $HgCl_2$) were tested to choose optimal condition for the BL reaction.

Different incubation times, from 0 up to 120 min, were tested, at room temperature, adding 20 µL of 1.00 µM $HgCl_2$ directly on wells with bacteria cells entrapped in agarose. Analytical

performance of the *E. coli* mercury-sensitive paper was evaluated adding a 20 µL-volume of different concentrations of $HgCl_2$, from $1.00x10^{-4}$ to 1.00 µM. As for β-gal paper, after a 60 min-incubation of *E. coli* sensor cells with different concentrations of $HgCl_2$, the Furimazine-paper was positioned, and the bioluminescent image was taken. Also, for *A. fischeri* toxicity paper, volumes from 5 to 25 µL of sample (1.00 µM $HgCl_2$) were tested and incubation times from 0 to 120 min to choose the optimal condition for *A. fischeri* to respond. An inhibition curve with different concentrations of $HgCl_2$ (from $1.00x10^{-4}$ to 1.00 µM) was performed to evaluate the LOD for *A. fischeri* toxicity paper.

Dimethyl sulfoxide (DMSO) was used as model toxic compound to investigate the biosensor response to toxic samples. Dose response curves were performed with DMSO dilutions ranging from 0.25 to 50%$_{v/v}$ prepared in ddH_2O.

All experiments were performed at least three times in triplicate. The LOD was calculated as the BL signal of the control (ddH_2O) plus three times the standard deviation.

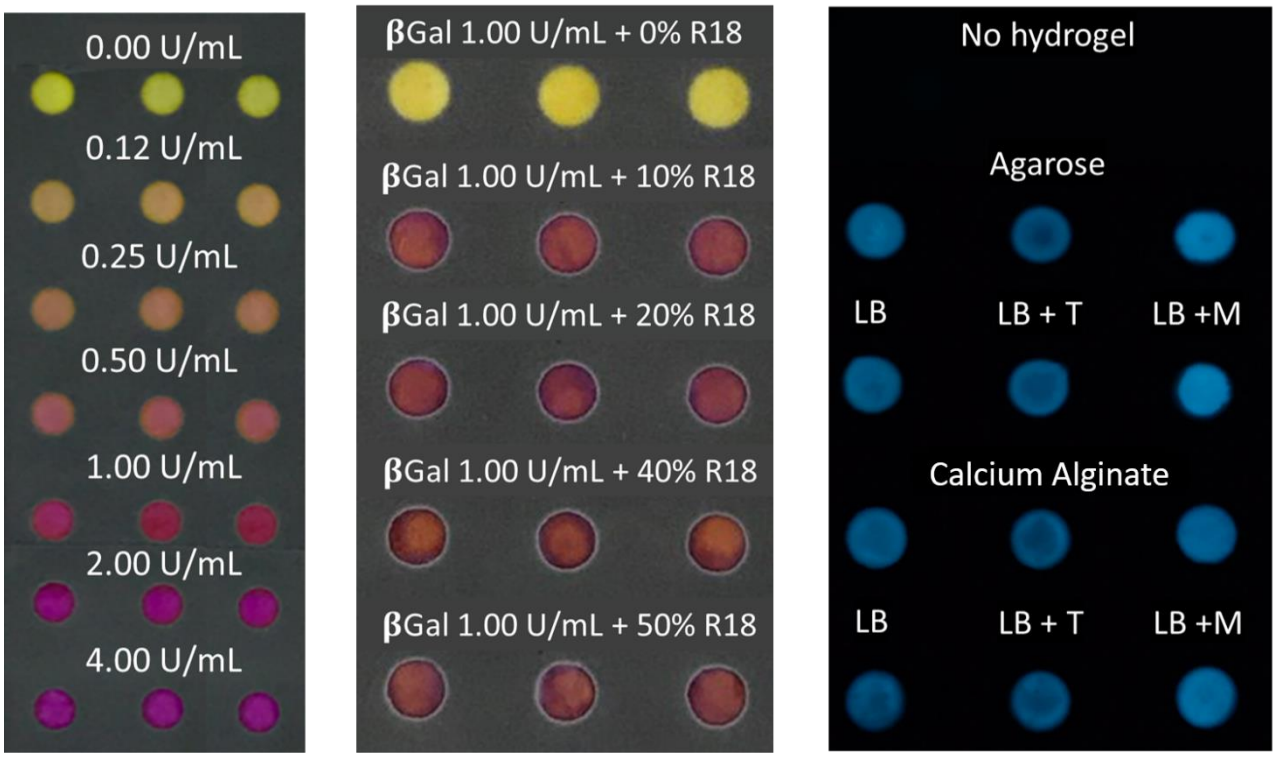

Figure S1. Optimization of ready-to-use paper-based biosensor with β-gal and BL bacterial sensors. C) Reflectance images of different β-galactosidase concentrations adsorbed on paper (from 0.0 to 4.00 U/mL) (left) and of the lyophilized β-galactosidase (1.00 U/mL) with different R18 medium percentages (concentration range from 0 to 50%$_{v/v}$) (center). BL images of *A. fischeri* immobilized on paper without hydrogel, with agarose (0.75%$_{w/v}$) and with calcium alginate (1.5%$_{w/v}$), supplemented with only LB (LB), LB plus trehalose (LB + T), and LB plus milk (10% v/v). (LB + M).

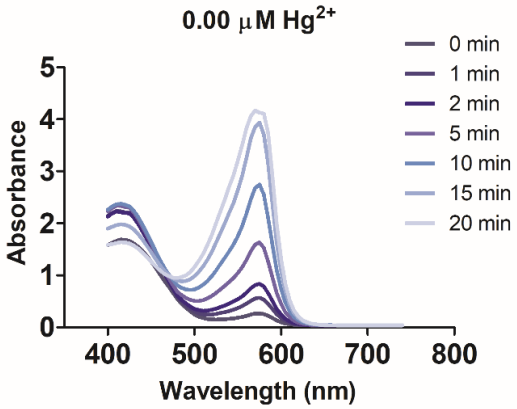
0.00 μM Hg2+
0 min
1 min
2 min
5 min
10 min
15 min
20 min
Absorbance
Wavelength (nm)

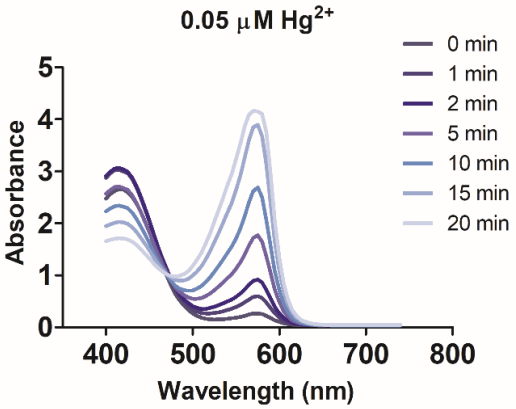
0.05 μM Hg2+
0 min
1 min
2 min
5 min
10 min
15 min
20 min
Absorbance
Wavelength (nm)

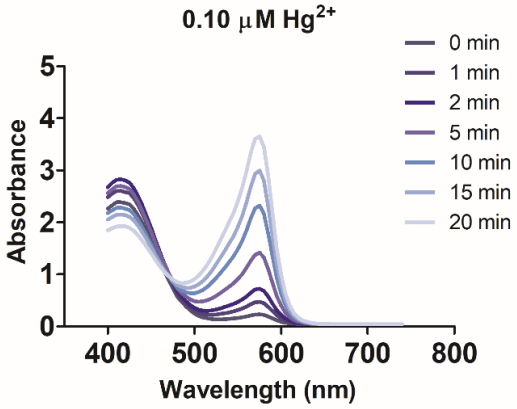
0.10 μM Hg2+
0 min
1 min
2 min
5 min
10 min
15 min
20 min
Absorbance
Wavelength (nm)

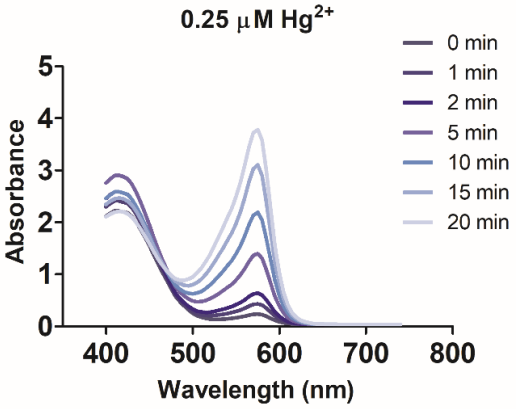
0.25 μM Hg2+
0 min
1 min
2 min
5 min
10 min
15 min
20 min
Absorbance
Wavelength (nm)

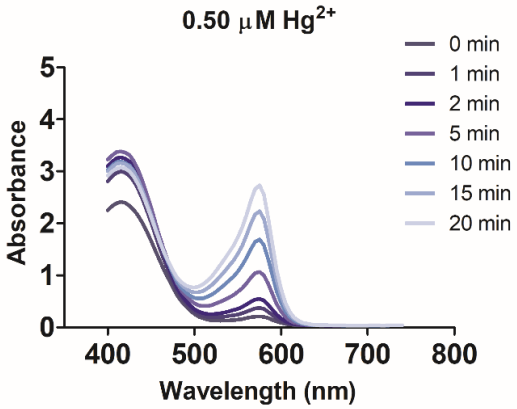
0.50 μM Hg2+
0 min
1 min
2 min
5 min
10 min
15 min
20 min
Absorbance
Wavelength (nm)

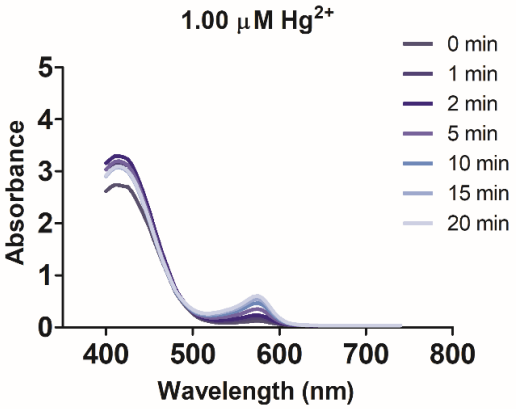
1.00 μM Hg2+
0 min
1 min
2 min
5 min
10 min
15 min
20 min
Absorbance
Wavelength (nm)

Figure S2. UV-Visible absorption spectra of β-gal paper with CPRG substrate. UV-Visible absorption spectra were obtained with Thermo Scientific™ Varioskan™ (from 0 to 20 min) with a fixed concentration of Hg^{2+}.

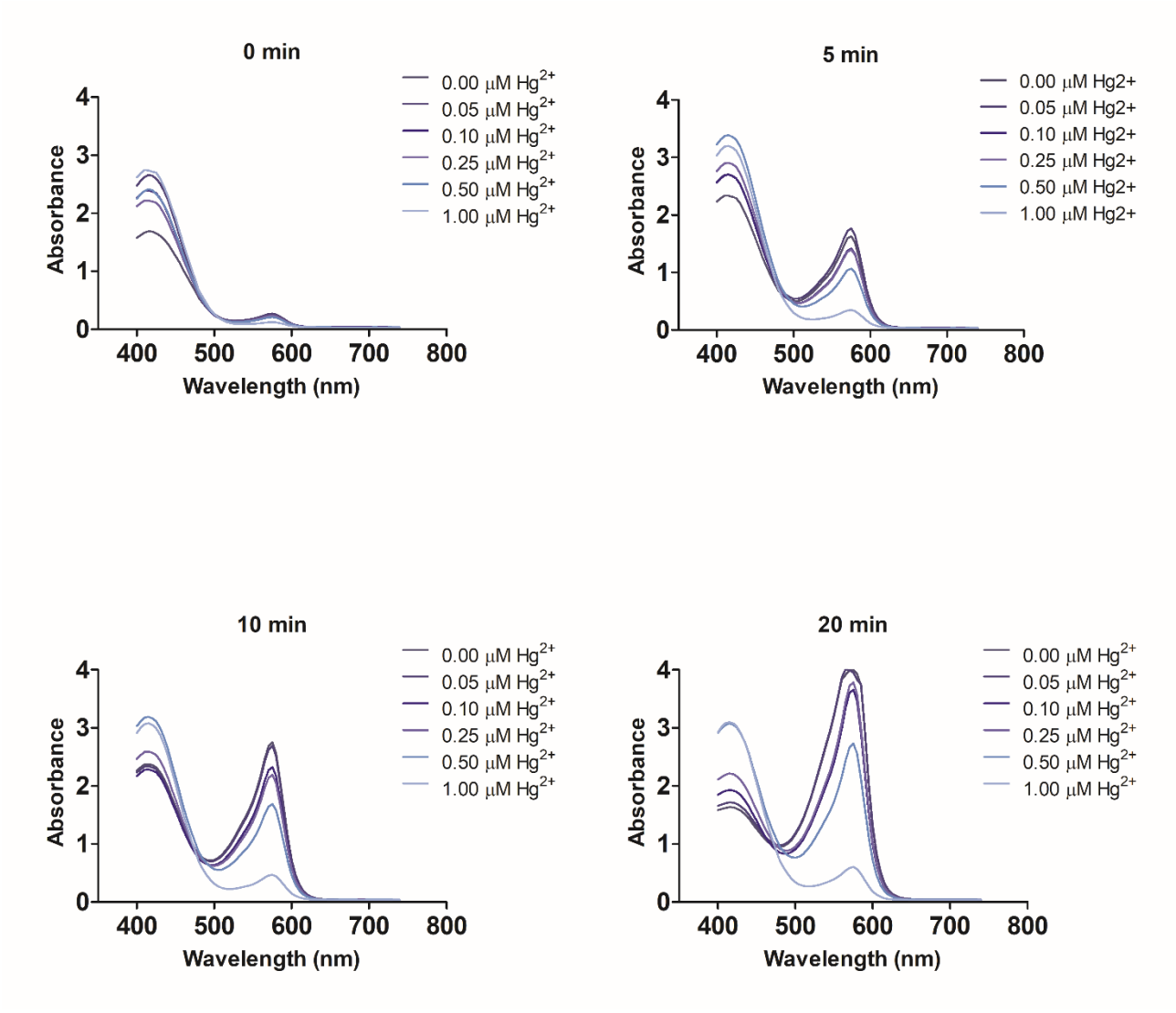

Figure S3. Optimization of β -gal/CPRG incubation time. UV-Visible absorption spectra of β -gal/CPRG in the presence of Hg2+ acquired with Thermo Scientific™ Varioskan™.

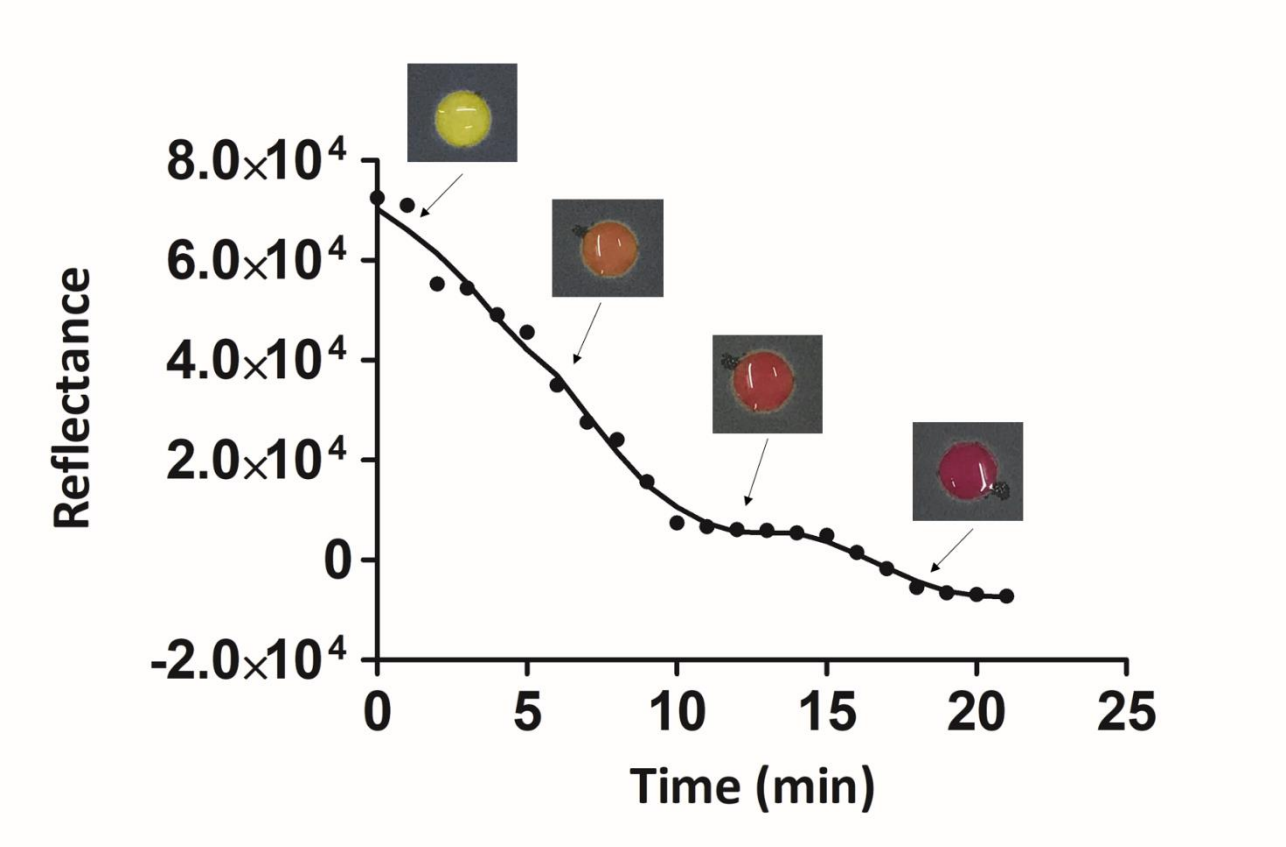

Figure S4. β-gal/CPRG reflectance kinetics on paper. Colour development over time with on-paper immobilised β-gal/CPRG. Reflectance images were taken with Oneplus 6T smartphone camera.

Table S1: Recovery of mercury (II) in lake water (n = 3). *n.d.:* not detectable

		BL detection			**COL detection**		
DMSO ($\%_{v/v}$)	**$HgCl_2$ (µM)**	**Found - Tox corrected (µM)**	**Recovery (%)**	**RDS (%)**	**Found (µM)**	**Recovery (%)**	**RDS (%)**
0	$5.00x10^{-3}$	$5.36x10^{-3}$ ± $5.89x10^{-4}$	107± 12	11	*n.d.*	*n.d.*	*n.d.*
	0.10	0.11 ± 0.01	111 ± 10	9	0.10 ± $8.00x10^{-3}$	101 ± 8	8
	0.25	0.22 ± 0.02	88 ± 8	9	0.27 ± 0.03	110 ± 13	12
	1.00	1.14 ± 0.09	114 ± 9	8	0.98 ± 0.08	98 ± 8	8
2.5	$5.00x10^{-3}$	$5.84x10^{-3}$ ± $6.31x10^{-4}$	117 ± 13	11	*n.d.*	*n.d.*	*n.d.*
	0.10	0.15 ± 0.02	150 ± 20	13	0.13 ± $9.00x10^{-3}$	128 ± 9	7
	0.25	0.28 ± 0.03	112 ± 12	11	0.30 ± 0.03	121 ± 13	10
	1.00	1.08 ± 0.09	108 ± 9	8	1.01 ± 0.08	101 ± 8	8
10	$5.00x10^{-3}$	$8.30x10^{-3}$ ± $7.20x10^{-4}$	1650 ± 143	8	*n.d.*	*n.d.*	*n.d.*
	0.10	0.13 ± $7.74x10^{-3}$	133 ± 8	6	0.92 ± 0.07	924 ± 70	7
	1.00	0.92 ± 0.11	91 ± 11	12	1.05 ± 0.09	105 ± 9	9
25	$5.00x10^{-3}$	*n.d.*	*n.d.*	*n.d.*	*n.d.*	*n.d.*	*n.d.*
	0.25	0.20 ± 0.03	81 ± 11	13	1.08 ± 0.10	431 ± 40	9
	1.00	0.74 ± 0.09	73 ± 9	12	1.11 ± 0.08	111 ± 8	7